

1 Uncovering gene-family founder events during major 2 evolutionary transitions in animals, plants and fungi 3 using GenEra

4

5 Josué Barrera-Redondo^{1,*}, Jaruwatana Sodai Lotharukpong¹, Hajk-Georg Drost^{2,*}, Susana M. Coelho^{1,*}

6

7 ¹Department of Algal Development and Evolution, Max Planck Institute for Biology, Max-Planck-Ring 5,
8 72076, Tübingen, Germany.

9 ²Computational Biology Group, Department of Molecular Biology, Max Planck Institute for Biology, Max-
10 Planck-Ring 5, 72076, Tübingen, Germany.

11 * To whom correspondence may be addressed.

12

13 *Running title: Gene-family founder events using GenEra*

14

15 Abstract

16 The emergence of new genes is an important driver of evolutionary novelty. Yet, we lack a conceptual
17 and computational approach that accurately traces gene-family founder events and effectively
18 associates them with trait innovation and major radiation events. Here, we present GenEra, a
19 DIAMOND-fuelled gene-family founder inference framework that addresses previously raised
20 limitations and biases of founder gene detection in genomic phylostratigraphy by accounting for
21 homology detection failure (HDF). We demonstrate how GenEra can accelerate gene-family founder
22 computations from several months to a few days for any query genome of interest. We analyzed 30
23 genomes to explore the emergence of new gene families during the major evolutionary transitions in
24 plants, animals and fungi. The detection of highly conserved protein domains in these gene families
25 indicates that neofunctionalization of preexisting protein domains is a richer source of gene-family
26 founder events compared with *de novo* gene birth. We report vastly different patterns of gene-family
27 founder events in animal and fungi before and after accounting for HDF. Only plants exhibit a consistent
28 pattern of founder gene emergence after accounting for HDF, suggesting they are more likely to evolve
29 novelty through the emergence of new genes compared to opisthokonts. Finally, we show that gene-
30 family founder bursts are associated with the transition to multicellularity in streptophytes, the
31 terrestrialization of land plants and the origin of angiosperms, as well as with the evolution of bilateral
32 symmetry in animals.

33

34 Introduction

35 Most protein-coding genes of extant organisms descend from a small set of founder genes that were
36 already present in the last universal common ancestor of all living systems (LUCA) (1,2). Evolutionary
37 novelty at the molecular scale is therefore thought to be largely driven by the duplication and
38 neofunctionalization of preexisting genetic information (3). Nonetheless, genomic studies carried out
39 throughout the last three decades show a pervasive number of cases of genes with limited or
40 untraceable gene homology (4–6). These taxonomically-restricted genes (TRGs) are protein-coding
41 genes that are present in a particular evolutionary lineage with no detectable homologs in other
42 organisms. The presence of TRGs is usually attributed to gene-family founder events, that is, the
43 emergence of the earliest common ancestor of an extant family of protein-coding genes (7). TRGs are
44 associated with the emergence of novel morphologies (8,9), immune defense mechanisms (10), and
45 ecological specialization (11) across the tree of life. Proposed mechanisms that explain the birth of new
46 gene families include neofunctionalization processes that modify the founder-gene beyond recognition
47 (4), the differential combination and fusion of protein folds and domains that predate LUCA (12), or *de*
48 *novo* gene birth from noncoding DNA (6). However, the extent to which TRGs can be attributed to gene-
49 family founder events has been extensively debated, since the lack of traceability of a gene can also
50 explain why some TRGs cannot be detected outside the evolutionary lineage under study (13–15). With
51 the advent of the Earth BioGenome Project, the scientific community is reaching a stage where
52 representative genomes will be available for a major portion of eukaryotic lineages (16). While
53 presented as an unparalleled opportunity to study the evolutionary processes that shape genes across
54 diverse evolutionary lineages (17), we lack a robust methodology and software solution to leverage
55 comparative genomics at tree-of-life scale and achieve high-confidence predictions of TRG and robust
56 assessment of gene birth events.

57 Genomic phylostratigraphy was initially introduced as a method to annotate gene founder events along
58 the tree of life, often represented by a taxonomic classification (7). Inferring the relative ages of genes
59 in a genome helps to address evolutionary questions such as the possible relation between the
60 emergence of TRGs and lineage-specific evolutionary novelties during major radiation events (18), how
61 ontogenetic transcriptional patterns evolve (19,20), whether new genes evolve faster compared to old
62 genes (21), or at what rate the emergence of completely novel proteins is driven by *de novo* gene birth
63 events (6). While conceptually powerful, several studies have questioned the detection sensitivity of
64 the phylostratigraphic approach (13–15,22). Gene ages may appear younger than they actually are due
65 to gene prediction errors in the target database (23). Previous approaches have also overlooked
66 contamination or horizontal gene transfer across lineages, which can overestimate a gene's age in a
67 given organism (24). Furthermore, they did not estimate gene ages in terms of gene families, but
68 assumed that dating individual genes extrapolates to the entire gene family (9,25). As such, the overall
69 number of gene founder events is prone to be conflated by the subsequent duplication of a founder
70 gene. Moreover, the computational burden of genomic phylostratigraphy limits its scalability. The
71 pairwise sequence aligner BLASTP (26) (a gold standard tool to search gene homologs against sequence
72 databases) is typically used for phylostratigraphic analyses (27,28). For phylostratigraphic applications,
73 BLASTP has been shown to perform equally well in reporting distant homologs when compared to
74 slower but more sensitive profile-based methods, such as HMMer (29) or PSI-BLAST (30) during the
75 inference of gene ages (28). While faster and equally reliable as several other tools (28), a BLASTP search
76 of a full set of organismal genes (approx. 5,000 to 40,000 genes) against currently available public
77 sequence databases can take up to several weeks or even months, limiting its scalability to hundreds

78 or thousands of species (17). Importantly, the greatest caveat of genomic phylostratigraphy is that small
79 and fast-evolving genes are often mis-annotated as young genes due to homology detection failure
80 (HDF), *i.e.*, the inability of pairwise local aligners to trace back distantly-related homologs only due to
81 neutral sequence divergence which results in spurious patterns of TRG birth (13,15). Overall, these
82 caveats undermine the power of the original phylostratigraphic method, motivating several authors to
83 propose key methodological improvements to obtain a more reliable estimate of gene-family founder
84 events (9,15,23,24,28,31,32).

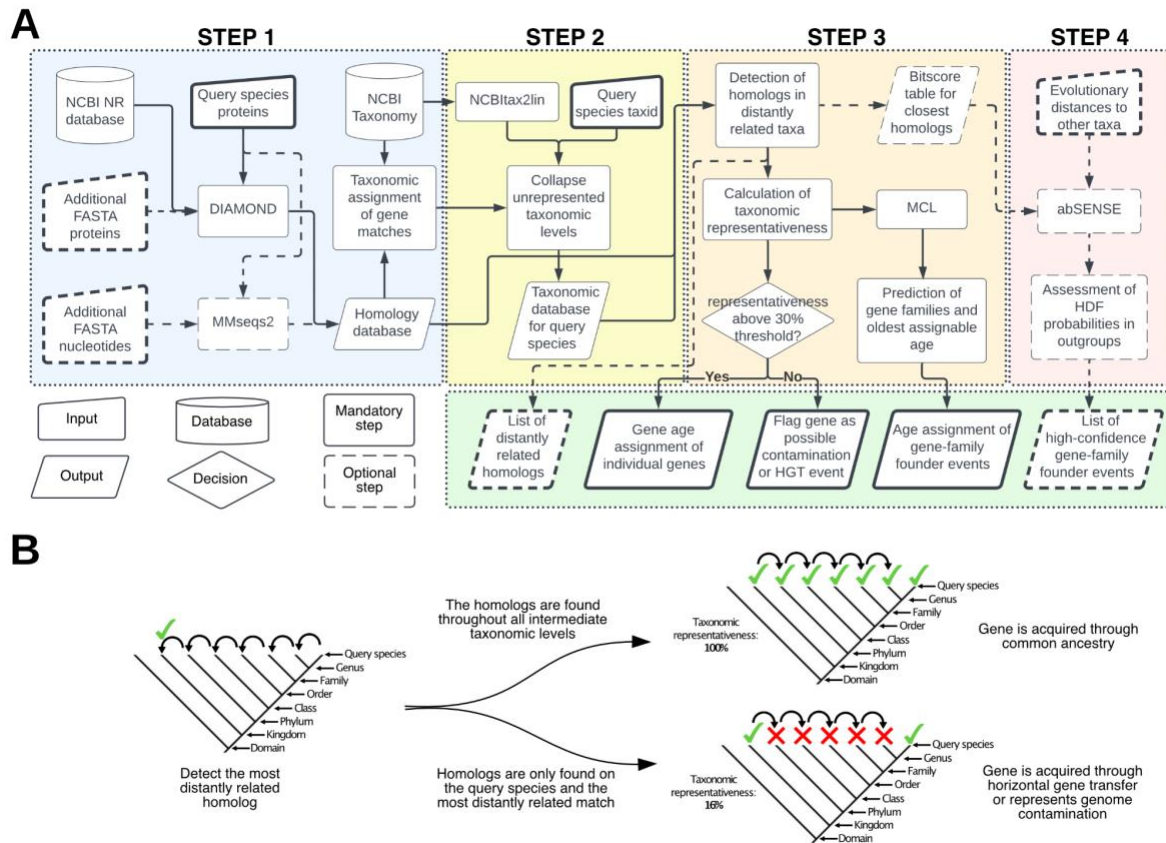
85 Here, we present a conceptually redesigned founder-gene inference method that employs the superior
86 computational speed of the protein aligner DIAMOND (17). This method draws from the principles of
87 genomic phylostratigraphy (7) to accurately pinpoint the evolutionary origin of gene families, but
88 extends its initial scope to account for founder gene-family origination events and sufficient homology
89 detection sensitivity. We apply this method to the reference genome of *Saccharomyces cerevisiae* (33)
90 to benchmark its scalability and accuracy when searching against thousands of target genomes. We use
91 our methodology to revisit the putative pattern of TRG emergence associated with important
92 evolutionary events in plants and animals, such as the transition to multicellularity in animals or the
93 terrestrialization event of plants (4). We also explore whether analogous TRG patterns are also present
94 in Fungi. Furthermore, we calculate and investigate the gene age maps of 30 genomes across vastly
95 different lineages within three different eukaryotic kingdoms to test whether accounting for HDF
96 changes the observed patterns of TRG emergence (15), as some radiation events may lead to a strong
97 signal of gene untraceability (34). Finally, we investigate the presence of ancient protein domains within
98 these TRGs to evaluate the relative contribution of gene duplication and domain reshuffling in TRG
99 emergence compared to *de novo* gene birth.

100 Materials and Methods

101 Addressing the previous shortcoming of genomic phylostratigraphy with GenEra
102 GenEra address all major limitations and scalability of previous phylostratigraphic approaches while
103 expanding its functionality by implementing a DIAMOND-fuelled method to detect gene-family founder
104 events (Fig. 1A). The pipeline can be used on the full set of genes from any species whose taxonomy is
105 included in the NCBI database (35). We provide this pipeline as an open source command line tool
106 called GenEra (<https://github.com/josuebarrera/GenEra>).

107

108



109

110 **Figure 1. Gene-family founder detection framework implemented in GenEra.** Overview of the pipeline for
 111 sensitive founder-gene family detection across the tree of life. A) Flowchart of the command-line tool GenEra.
 112 Solid arrows/elements represent the mandatory steps in the pipeline, while the dashed arrows/elements
 113 represent optional steps to enrich the results. B) Graphic representation of the rationale behind the taxonomic
 114 representativeness score (see Methods). GenEra first performs a taxonomic trace-back to determine the most
 115 distantly related homolog to a query species, and then tracks back the presence of homologs in all the
 116 intermediate taxonomic levels, which helps to detect putative contaminants in the query proteome, horizontal
 117 gene transfer events between increasingly distantly related taxa, or false positive matches.

118

119 The first step of GenEra replaces BLASTP with the ultra-fast and sensitive protein aligner DIAMOND,
 120 which has recently been extended for ultra-sensitive gene similarity assessments at tree of life scale
 121 (17). By default, BLAST and other sequence search algorithms limit the maximum number of top
 122 sequence hits that are reported in the analysis to the 500 best hits, which is an often overlooked
 123 limitation that hinders the extent by which genes can be traced back to distantly related taxa. With
 124 exponentially growing sequence databases covering hundreds of thousands of species, 500 top hits can
 125 at best cover only 500 different subject species, thereby losing a significant proportion of age-
 126 assignable information. Using DIAMOND instead of BLAST allows us to build a customized list of pairwise
 127 alignments against the entire NCBI non-redundant (NR) protein database, which harbors tens of
 128 thousands of genomes, alongside other user-defined protein datasets with an unlimited amount of
 129 sequence hits, generating results up to 8,000 times faster than BLASTP-based approaches while
 130 reaching the same level of accuracy (Fig. S1) (17). We established an e-value threshold below $1e^{-5}$ for a
 131 sequence hit to be considered a reliable true positive. The choice of this threshold was based on an
 132 extensive threshold-robustness study to test the influence of a diverse range of e-values on gene age
 133 assignments with the ultimate aim to determine the most robust e-value threshold when running

134 GenEra in default mode. Indeed, a less stringent threshold does not improve the age assignment of
135 genes and may lead to an increased rate of false positive age assignments, given the size of the NR
136 database, while more stringent thresholds lead to an overestimation of TRGs (Fig. S2). Another issue
137 raised for genomic phylostratigraphy is that spurious genome annotations or comparison between
138 annotations with different levels of quality and accuracy can overestimate the proportion of recently-
139 evolved proteins in the analysis (23,31). To address this short-coming, GenEra is able to include an
140 additional protein-against-nucleotide search through MMseqs2 (36) with its most sensitive parameters
141 ($s = 7.5$) to reconfirm gene age assignments with an annotation-free approach solely based on six-frame
142 alignments. Using GenEra with genome assemblies in parallel with protein annotations (Table S1)
143 significantly reduces the number of TRGs in the youngest taxonomic levels, from the species-level up
144 to the genus-level age assignments, but older taxonomic levels seem largely unaffected when including
145 protein-against-nucleotide data (Fig. S3).

146 The second step of GenEra employs NCBItax2lin (available via <https://github.com/zyxue/ncbitax2lin>) to
147 generate a lineage database that is used to associate the NCBI Taxonomy ID in the list of DIAMOND
148 pairwise alignments with their hierarchical taxonomic identity in the NCBI Taxonomy database. The
149 NCBI Taxonomy is a curated database that reflects the current knowledge of the relationships between
150 all known organisms (35). Hence, each taxonomic level in the lineage database corresponds to a
151 monophyletic group in a species tree. This allows GenEra to determine the evolutionary relationship
152 between the matching genes from the sequence database and the query species. The lineage database
153 that is generated by NCBItax2lin is not arranged in a hierarchical order, given that the taxonomic ranks
154 are usually asymmetrical between different lineages in the NCBI Taxonomy database (37). Thus, GenEra
155 retrieves the correct taxonomic order from the NCBI server to rearrange the lineage database in a
156 hierarchical order, in accordance with the taxonomic levels that are reported in the NCBI for the query
157 species. Given the historical scopes and interests of the scientific community during the era of high-
158 throughput sequencing, current genomic databases are still biased toward having sequencing data for
159 certain groups of organisms, while having no publicly available genomes for others (38). This
160 complicates the detection of gene-family founder events, since having genomic data is required to
161 assign a gene to a certain age in a reliable and systematic manner. To address this issue, GenEra
162 searches the entirety of sequence matches that were retrieved with DIAMOND and only retains the
163 taxonomic levels for which at least one representative species matches more than 10% of the proteins
164 in the query species for further analyses. This threshold was empirically established to exclude the
165 organisms in the NR that are represented by only a few genes and not by genomic data (Fig. S4).

166 The third step of GenEra performs a taxonomic trace-back to determine the most distantly-related
167 lineage that matches each gene of the query species (Fig. 1B). Once the most distant homolog for a
168 query protein is found, the pipeline calculates a taxonomic representativeness score to estimate the
169 reliability of assigning a gene age based on this sequence match. The rationale for this procedure is to
170 address another limitation of the original genomic phylostratigraphy, where the most distant hit was
171 not reconfirmed at higher taxonomic levels but rather assumed, which created a systematic bias when
172 dealing with contamination and horizontal gene transfer events. GenEra reconfirms hits at higher levels
173 using a taxonomic representativeness metric (L) which is calculated as the presence of homologs in at
174 least one representative species for each of the intermediate taxonomic levels between the most
175 distantly-related lineage and the query species (Fig. 1B). The number of internode taxonomic levels
176 with representative gene homologs (RP) is divided by the total number of taxonomic steps that separate
177 the most distantly-related match from the gene of the query species (AP), while excluding the youngest

178 taxonomic level (usually the species level), since the presence of the gene in the query species already
179 confirms its representativeness at that level:

$$180 \quad L = 100 * (RP / (AP - 1))$$

181 This gives a taxonomic representativeness score L with a scale from 100 to $100 * (1 / (AP - 1))$, which helps
182 to flag genes that are only present in the query species and in other distantly related taxa (Fig. 1B).
183 Genes with a low taxonomic representativeness are discordant with the concept of synapomorphy (39),
184 where a homologous character (in this case, a gene) should be inherited to all the taxa that share a
185 common ancestor. However, secondary losses of inherited genes should be expected to happen
186 throughout the tree of life. Thus, the taxonomic representativeness score can be influenced by gene
187 loss events in the genomes that act as representatives in the intermediate taxonomic levels, or due to
188 the availability of only scarce and low-quality genomic data at certain taxonomic levels. To address this
189 issue, we established a relaxed taxonomic representativeness threshold of 30%, so that only genes with
190 a particularly low score are flagged as putative horizontal gene transfer events, contaminant sequences
191 in the assembly that do not belong to the query species, or false positive matches against the database
192 (Fig. S5). This score is reported for every gene in the query species, and the user can also establish a
193 custom threshold that is appropriate for the dataset and taxon of interest.

194 GenEra can optionally report the best sequence hit (as defined by its bitscore) that can be assigned to
195 the oldest taxonomic level for each query gene. This feature helps users to identify erroneous gene age
196 assignments due to false positive matches, and to manually evaluate genes with a low taxonomic
197 representativeness. This feature also helps to identify candidate non-coding sequences from which
198 potential *de novo* TRGs could have emerged when implementing a protein-against-nucleotide search.

199 Once all the genes in a query species have been assigned to a certain age, GenEra performs an all-vs-
200 all DIAMOND search of the query proteins against themselves to detect paralogs within the genome of
201 the query species. The e-values of the all-vs-all DIAMOND search are normalized through a negative
202 log₁₀ transformation, and are subsequently used for a clustering analysis with an inflation value of 1.5
203 to predict gene families using MCL (40). GenEra uses the oldest assignable gene age for each of these
204 gene clusters to estimate the number of gene-family founder events throughout the evolutionary
205 history of the query species.

206 GenEra has a fourth additional step to assess whether the gene age assignment of the query genes can
207 be explained by HDF. Bitscores obtained through pairwise sequence alignments have been shown to
208 decay exponentially as a function of evolutionary distance (15). Given enough data points, one can
209 calculate the expected bitscore for a given gene in a distantly related species when such gene is not
210 detected, and hereby calculate the probability of not finding this gene as a consequence of bitscore
211 decay alone (15). When GenEra is given a list of pairwise evolutionary distances (*e.g.*, substitutions per
212 site in a phylogenetic tree) between the query species and other taxa in the database, it searches for
213 the closest homolog in these species, which are defined as the highest bitscore matches to each of the
214 query genes. GenEra uses the bitscore of these genes to calculate HDF probabilities using abSENSE (15)
215 for all the species that lack any traceable homolog to each query gene in the target species. GenEra can
216 use these probabilities to test the null hypothesis of untraceable homology for each gene that is
217 assigned to a given taxonomic level. The ability of GenEra to test HDF for each taxonomic level is
218 dependent on the taxonomic sampling that is given by the user, which is determined by the taxonomic
219 sampling of the phylogeny that is used to calculate the evolutionary distances. Hence, the use of
220 phylogenies at different taxonomic levels can be used by GenEra to test for HDF in gene-family founder

221 events at different evolutionary scales. Once a gene is assigned to a certain age, GenEra analyzes the
222 HDF probability of the closest species (as defined by their evolutionary distance to the query species)
223 that belongs to the next taxonomic level, and labels the gene age assignment as a high-confidence gene
224 founder event whenever the HDF probabilities fall below 0.05 in the outgroup (Fig. S6). Thus, GenEra
225 can make an informed decision on whether the gene age assignments can be explained by gene-family
226 founder events or through sequence divergence alone that make these genes untraceable given their
227 size and substitution rate (27).

228 Assessment of gene-family founder events in 30 eukaryotic genomes

229 We downloaded representative genomes of plants, animals and fungi from the Uniprot reference
230 proteomes to study the patterns of gene-family founder events throughout these major eukaryotic
231 lineages by using GenEra (Table S2). We chose 10 representative taxa across the taxonomic diversity
232 of each of these three kingdoms to revisit the previously observed peaks in gene-founder events
233 associated with the diversification of animals and land plants (4), and to determine whether this same
234 pattern arises in Fungi. We collapsed the Eumetazoan taxonomic level (i.e. all animals excluding
235 Porifera) from our animal analysis, since recent evidence indicates that Eumetazoa is paraphyletic (41).

236 We extracted the evolutionary distances from previously reported phylogenies using the ape package
237 in R (42) to calculate HDF probabilities at different taxonomic levels and evaluate the proportion of
238 gene families that can be confidently assigned to gene-family founder events. For the Fungi kingdom,
239 we used 81 evolutionary distances from a maximum likelihood tree (43) encompassing several
240 evolutionary distances from our 10 target genomes (Table S3), including *Fonticula alba* and other
241 opisthokonts as outgroups to test gene-family founder events up until the Fungi level. For Metazoa, we
242 used 43 evolutionary distances from a posterior consensus bayesian tree (41) comprising a large portion
243 of the animal phyla (Table S4) and which includes *Monosiga brevicollis* and *Salpingoeca rosetta* as
244 outgroups (44) to test gene founder events at different taxonomic levels up to Metazoa. For
245 Embryophyta, we used 61 evolutionary distances (Table S5) from a posterior consensus bayesian tree
246 (45) that incorporates several plant genomes, as well as green algae and red algae, which helped us
247 test gene-family founder events up until the Viridiplantae level. All the gene families who had HDF
248 probabilities < 0.05 in the closest outgroup were considered as high-confidence TRGs that resulted from
249 gene-family founder events.

250 Results

251 By improving genomic phylostratigraphy with a gene family clustering strategy and HDF tests, we were
252 able to estimate the number of putative gene-family founder events throughout the plant, animal and
253 fungal lineages. We used 10 genomes for each of these lineages to evaluate the common patterns of
254 putative gene founder events that have been previously described using genomic phylostratigraphy
255 with single genomes (4). All our results are available as supplemental data.

256 Before calculating HDF probabilities, we found a consistent overrepresentation of putative gene-family
257 founder events at the taxonomic levels that correspond to the crown node of land plants, animals and
258 fungi (Fig. 2). These gene age peaks were observed independently of the taxonomic lineage from which
259 the species belong within their kingdom, revealing a common evolutionary signal. We found no
260 evidence of whether this convergent pattern was correlated with the number of available genomes in

261 the database at those taxonomic levels, as these levels can have a vastly different number of
262 representative genomes depending on the species that is analyzed (Table S6).

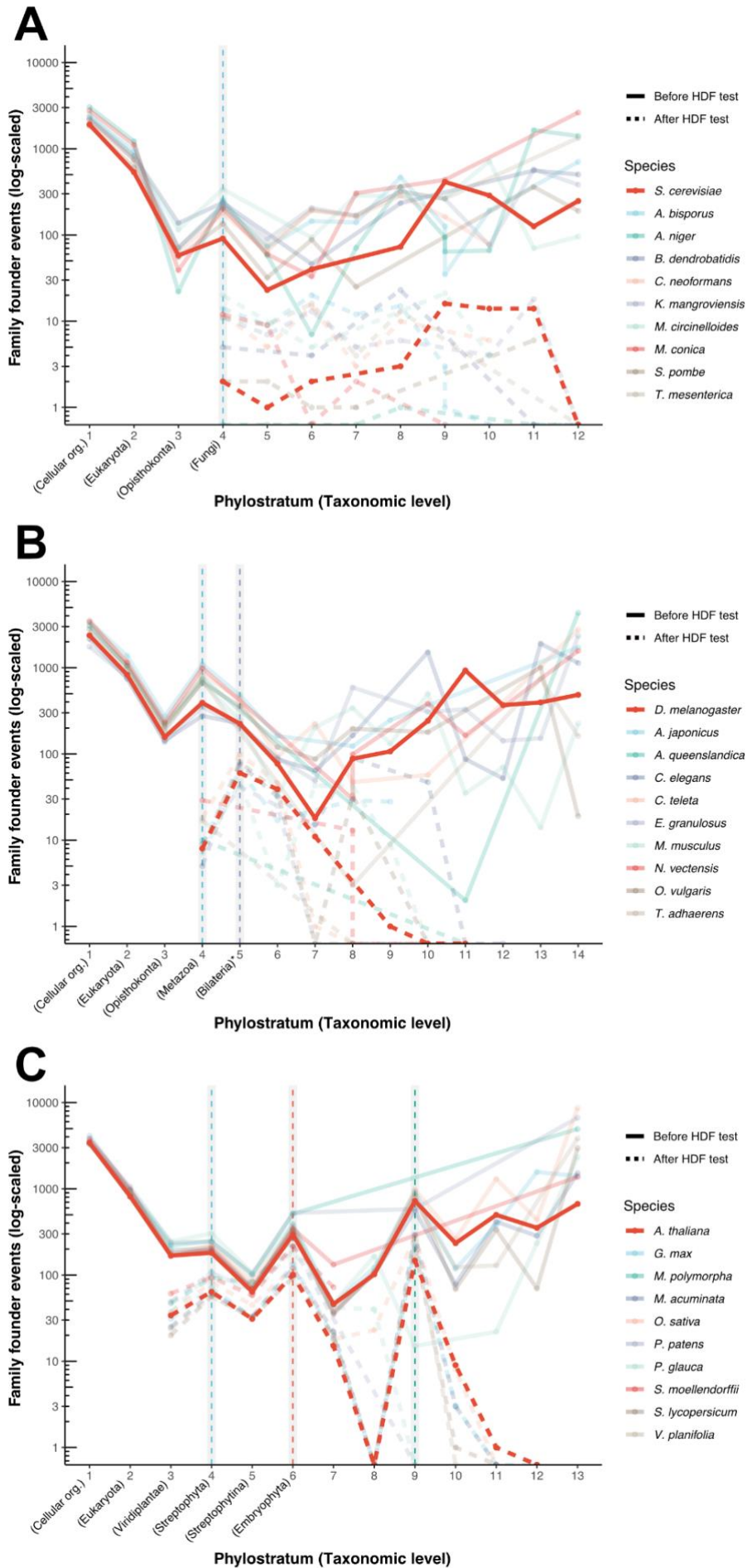
263 However, the patterns of gene-family founder events considerably change after filtering the dataset by
264 HDF probabilities. The total number of putative founder events diminished between one and two orders
265 of magnitude in all the analyzed species after retaining only high-confidence gene ages that could not
266 be explained by HDF. Fungi lost any discernible pattern of gene emergence that could be traced back
267 to a particular evolutionary transition after accounting for HDF, including the putative TRG
268 overrepresentation at the kingdom level (Fig. 2A). Likewise, the signal associated with the emergence
269 of Metazoa is lost in the high-confidence gene-family founders, but the transition to bilateral symmetry
270 (Bilateria) is consistently enriched in high-confidence gene-family founder events on all the bilateral
271 animals in our dataset (Fig. 2B). We analyzed the biological function of these TRGs by looking at the
272 gene annotation of *D. melanogaster*. We detected the emergence of the Ninjurin A-C genes, the
273 *disconnected* gene, the Dampened gene and the gene family composed of the Gurken, Keren and spitz
274 genes.

275 The patterns of gene-family founder events in plants remained fairly consistent despite predicting a
276 vastly smaller amount of founder events. The most consistent bursts of gene-family founder events in
277 plants were found in Streptophytes when green algae transitioned to complex multicellularity (46), in
278 embryophytes when plants conquered the land (47), and in angiosperms, when plants evolved flowers
279 (48) (Fig. 2C). We inspected the gene annotations of *A. thaliana* to evaluate the biological function of
280 these TRGs.

281 Some of the successful gene-family founder events that were identified as high-confidence
282 Streptophyta TRGs include a family of Basic Helix-Loop-Helix (bHLH) transcription factors (49), the
283 COBRA-like gene family that act as key regulators of cell-wall expansion in the meristems (50), a family
284 of auxin canalization proteins that regulate plant growth through auxin transport (51) and the
285 BRASSINAZOLE-RESISTANT family of transcription factors that modulate brassinosteroid signaling in
286 plants (52). Surprisingly, ARABIDILLO and the ULTRAPETALA gene families appear to be Streptophyta
287 TRGs, with putative homologs in the charophyte algae *Klebsormidium nitens* (GAQ84482.1 and
288 GAQ90507.1, respectively).

289 The high-confidence gene-family founder events that were linked to the emergence of embryophytes
290 include a family of F-box/kelch-repeat proteins that regulate the biosynthesis of phenylpropanoids (53),
291 the group 2 of late embryogenesis abundant (LEA) proteins that are involved in plant response to
292 osmotic and oxidative stress due to desiccation (54), two groups of bHLH transcription factors (49), a
293 gene family that contains MORPHOGENESIS OF ROOT HAIR 6 (MRH6), a gene family that contains
294 Piriformospora indica-insensitive protein 2 (PII-2), the SOSEKI gene family that regulates cell polarity in
295 early plant development (55) and the LONGIFOLIA gene family, involved in leaf development (56).

296 Within the gene-family founder events in angiosperms, we found class III of Ovate family proteins (OFP)
297 and the family of paclobutrazol resistance (*PRE*) genes. However, most of the TRGs in this taxonomic
298 level belong to genes that are uncharacterized in *A. thaliana*. The founder event of the MADS-box gene
299 family was detected in LUCA.



301 **Figure 2. Detection of gene-family founder events at major evolutionary transitions in plants, animals and fungi.**
302 Overlapping plots of gene-family founder events before and after accounting for HDF (solid lines and dashed lines,
303 respectively). The taxonomic hierarchies that are shared between all the species are named in the X axis, while
304 the taxonomic levels that differ between species are just ranked by number. A) Fungi genomes with *S. cerevisiae*
305 as the representative species in the plot. The taxonomic level leading to the emergence of Fungi exhibits a burst
306 of gene-family founder events before the HDF test (dashed blue line), but all the common patterns are lost after
307 accounting for HDF. B) Animal genomes with *D. melanogaster* as the representative species in the plot. The
308 taxonomic level leading to the emergence of Metazoa also shows a burst of gene-family founder events before
309 the HDF test (dashed blue line). The Metazoa burst fades after accounting for HDF, but the taxonomic level of
310 Bilateria exhibit a burst after the HDF test for all bilaterian animals (*i.e.*, excluding *N. vectensis*, *T. adhaerens* and
311 *A. queenslandica*; dashed grey line). C) Plant genomes with *A. thaliana* as the representative species in the plot.
312 Plants genomes display a consistent pattern of gene-family founder events before and after accounting for HDF,
313 with gene-family founder bursts associated with the emergence of multicellularity (Streptophyta, blue dashed
314 line), the conquest of land by plants (Embryophyta, red dashed line) and the origin of flowering plants
315 (Magnoliopsida, green dashed line).

316 Discussion

317 Gene founder events facilitate evolutionary innovations. Determining the timing of these events is
318 therefore important for evolutionary research. Such inference is not trivial, since previous attempts to
319 estimate TRG birth have overlooked the effects of HDF (4,7–9,18). While these initial efforts were useful
320 for investigating more general processes of evolution, such as the assessment of transcriptome age
321 during development (19,20), they lack the detection sensitivity to decouple founder events of entire
322 gene families from patterns of gene untraceability. For this reason, we developed GenEra to provide
323 the community with a sensitive and computationally optimized approach for gene-family founder
324 detection across the tree of life. To demonstrate the versatility of GenEra, we analyzed 30 genomes
325 from plants, animals and fungi to capture the broad diversity of gene-family founder events in these
326 lineages. We show that GenEra is applicable to any eukaryotic genome and we provide extensive
327 documentation to facilitate its swift adoption in the life science community.

328 The origin of TRGs has sparked important debates over the last decade regarding the processes of gene
329 birth (4–6,13–15,22,27). A high proportion of gene age assignments in our dataset could be explained
330 by HDF, as previously reported (13–15). It is important to acknowledge that gene age assignments that
331 fail the HDF test should not be interpreted as not belonging to their estimated taxonomic level, but
332 rather that we cannot reject the null hypothesis of untraceable homology in more distantly related
333 lineages (15). This is particularly true for short and fast-evolving genes, which are prone to fail the HDF
334 test (15), but which are also more likely to have arisen recently, given that previously validated *de novo*
335 genes are usually shorter and have fewer exons compared to old genes (11,57). Nevertheless, the
336 probability of proteins to independently acquire similar tertiary structures *de novo* is astronomically
337 small, given that the number of possible amino acid configurations of a 100-residue protein that is
338 considered “small” (58) (20^{100} configurations) is bigger than the estimated number of atoms that are
339 contained in the observable universe ($\sim 10^{82}$ atoms) (2). Hence, finding conserved motifs and domains
340 outside the boundaries of TRGs should be regarded as compelling evidence to discard *de novo* birth
341 scenarios. The vast majority of the high-confidence TRGs we detected contain highly conserved protein
342 domains and motifs that are consistently found throughout the tree of life. Such is the case for the
343 bHLH motif, which can be found in transcription factors of all eukaryotes (59), the DIX domain in SOSEKI
344 genes that are also conserved throughout eukaryotes (55), the ARMADILLO repeat domain in

345 ARABIDILLO genes that can be found in animals (60) or transmembrane domains found throughout all
346 cellular organisms (61). These TRGs cannot be explained by HDF (13,15), nor through *de novo* gene
347 birth, as previously suggested (5). Our observations support the idea of gene duplication (3) and of
348 protein modularity, where gene-founder events result from the differential fusion of pre-existing folds
349 and domains (12), whose tertiary structure acquired the property to fold during the postulated era of
350 the RNA and peptide world (1,2). These domain-containing TRGs were coincidentally found as multi-
351 copy gene families, suggesting that old protein folds and domains were already optimized by natural
352 selection to perform their biological activity (1,2), ensuring the evolutionary success of these TRGs.
353 Despite the minor role of *de novo* gene birth in TRG emergence, the study and validation of successful
354 *de novo* founder events should be of particular interest for evolutionary research, as these events can
355 help us uncover the foundations of evolutionary novelty at the molecular level (62).

356 Our results before the HDF test retrieved analogous peaks of gene age assignments in plants and
357 animals that have been previously described by Tautz and Domazet-Lošo (4) and could extend their
358 insights by detecting a kingdom-level peak in Fungi. The consistency of these peaks throughout several
359 species with vastly different evolutionary histories and biological traits (*e.g.*, free living organisms and
360 parasites, unicellular and multicellular fungi, plants with haploid-dominant and diploid-dominant life
361 cycles, bilateral-symmetric and non-bilateral-symmetric animals) and the lack of a correlation between
362 the database and gene age assignment (Fig. S7) points towards a biological basis of such a convergent
363 pattern. However, the biological interpretation of TRG patterns should be taken with caution. These
364 TRG peaks have been previously interpreted as bursts of genomic novelty that have accompanied some
365 important diversification events throughout the evolutionary history of these lineages (4,9), but we
366 found that the overrepresentation of TRGs at the emergence of animals and fungi disappears after
367 accounting for HDF, suggesting that these peaks may be driven by untraceable homology beyond those
368 taxonomic levels (15), rather than gene-family founder events or any other source of molecular novelty.

369 The emergence of animals and fungi are associated with their independent emergence of
370 multicellularity (63) and the diversification bursts that followed this key evolutionary innovation (34).
371 Diversification events have long been known to correlate with molecular substitution rate accelerations
372 (64–66), even though the exact causal relationship between both phenomena remains underexplored
373 (67). If substitution rates are correlated with diversification events, we would expect a large proportion
374 of the genes in the genome to become untraceable beyond these major diversification bursts.
375 Accordingly, our analyses show a pattern of gene untraceability that is linked to the emergence and the
376 diversification bursts of these two eukaryotic kingdoms. Therefore, we propose that these gene age
377 assignment peaks are driven by substitution rate accelerations that were linked to the diversification
378 bursts that accompanied these major evolutionary transitions in animals and fungi. Although gene
379 emergence likely played an important role during these evolutionary transitions in the tree of life, our
380 results indicate that gene-family founder events may not be as pervasive in the emergence of
381 evolutionary novelties such as multicellularity in opisthokonts compared to the co-option of ancient
382 gene families that already existed in LUCA, such as transcription factors, cell-adhesion proteins and cell-
383 signaling genes, which likely drove biological novelty through novel regulatory pathways (68,69).
384 Furthermore, recent studies suggest multiple origins of multicellularity in Fungi through vastly different
385 evolutionary processes compared to animals or plants (69). This likely blurs any common pattern
386 between molecular innovations and the transition to multicellularity in fungi. A more in-depth analysis
387 of fungal genomes might elucidate key gene-family founder events in this eukaryotic lineage.

388 We found a consistent overrepresentation of gene-family founder events in Bilateria. The emergence

389 of Bilateria is defined by a change in developmental patterns that resulted in the evolution of bilateral
390 symmetry. Among our reported gene-family founder events, we found Gurken, spitz and Dampened as
391 Bilateria TRGs. These genes are all involved in the establishment of the anterior-posterior and dorsal-
392 ventral polarities and neurogenesis during development (70–72). Likewise, the protein *disconnected* is
393 involved in the formation of the nervous system and the connection of the visual nerve to the brain
394 (73).

395 Our results show that three major evolutionary transitions in plants are associated with the evolution
396 of entire new gene families. The observed pattern of TRG birth in plants is conserved even after
397 accounting for HDF, suggesting that plants are prone to evolve novel traits through the emergence of
398 new genes. The frequency of gene-family founder events in plants could be driven by the propensity of
399 their genomes to undergo structural rearrangements and whole-genome duplications (74). Our results
400 are consistent with an orthogonal approach by Bowles et al., where they find an independent burst of
401 gene novelty in the branch leading to Streptophyta and Embryophyta (8), even though that study did
402 not account for HDF, which likely inflated the amount of predicted TRGs at those taxonomic levels.
403 Streptophytes, which include land plants and charophytes, have been proposed to share a common
404 emergence of complex multicellularity (8,46). Complex multicellularity has been linked with the
405 expansion of transcription factors, the emergence of an internal communication system between cells
406 (63) and, in the case of plants, the emergence and expansion of cell-wall remodeling proteins (46).
407 Coincidentally, our analysis detected gene-family founder events in bHLH transcription factors (49),
408 BRASSINAZOLE-RESISTANT transcription factors (52), COBRA-like genes (50) and auxin canalization
409 proteins (51). Furthermore, the emergence of auxin canalization proteins and BRASSINAZOLE-
410 RESISTANT genes likely contributed to the establishment of an internal communication system between
411 cells in multicellular streptophytes through the regulation of the basic hormone-receptor systems that
412 predate the evolution of multicellularity (75). We found a putative ULTRAPETALA and ARABIDILLO
413 homologs among charophyte algae, even though these gene families were previously reported as
414 embryophyte and angiosperm TRGs, respectively (60,76). ARABIDILLO genes have been co-opted to
415 modulate different developmental processes in plants through abscisic acid signaling (60), while
416 ULTRAPETALA genes interact with the trithorax group of angiosperms to coordinate flower
417 development through chromatin-dependent transcriptional regulation (76). If the homologs found in
418 *Klebsormidium nitens* are reliable, this would suggest an early role of ULTRAPETALA and ARABIDILLO
419 homologs in streptophyte evolution (77).

420 The evolution of land plants (Embryophyta) is intertwined with an increased morphological complexity
421 compared to other streptophytes. The emergence of SOSEKI genes probably conferred plants with cell-
422 polarization mechanisms to ensure the correct development of complex multicellularity (55). The
423 LONGIFOLIA gene likely played an additional role in the emergence of complexity in land plants through
424 the development of leaves (56). The emergence of embryophytes has also been associated with the
425 emergence of several defense mechanisms to cope with the abiotic stresses that characterize the
426 transition from water to land, such as ultraviolet (UV) radiation, drought and temperature fluctuations
427 (47). Accordingly, we found a F-box/kelch-repeat gene-family founder event in Embryophyta, whose
428 gene members regulate phenylpropanoid biosynthesis (53). The production of phenylpropanoids has
429 long been recognized as a crucial adaptation in plants that allowed them to survive the effects of UV
430 radiation in land (47). The emergence of group 2 LEA proteins would have helped plants to cope with
431 drought stress (54) as they transitioned from water to land. The role of rooting structures and its
432 association with mycorrhizal fungi have also been proposed as important innovations in land plants

433 (47). We detected two bHLH groups in our analysis, which have been shown to coordinate the
434 development of rhizoids and roots in plants (78). We also detected MRH6 as an embryophyte TRG,
435 which is involved in root hair development (79). Furthermore, PII-2 is known to promote plant growth
436 and seed production through its interaction with the mycorrhizal fungus *Piriformospora indica* (80),
437 whose detection as an embryophyte TRG supports the role of plant-fungus interactions in the transition
438 from water to land (47).

439 The emergence of flowers and fruits are major evolutionary innovations in angiosperms that changed
440 the ecological dynamics of terrestrial life (48). Many genes that regulate flower development are known
441 to belong to old gene families, such as the MADS-box genes (81). Accordingly, our analysis retrieved
442 the founder event of MADS-box genes in LUCA. However, our results also detected the founder event
443 of the class III OFP genes, which are also involved in the development of fruits (82). Most of the founder
444 events we detected angiosperms belong to uncharacterized genes with unknown biological activity.
445 The experimental study of these TRGs should shed light on the evolution of flowering plants.

446 The consistency of our results with previous studies on the emergence of these widely studied
447 evolutionary transitions highlights the power of GenEra to accurately detect molecular innovations in
448 three different eukaryotic lineages. Our method is expected to be a useful resource to detect novel
449 gene-family founder events on other important transitions throughout the tree of life.

450 Funding

451 This work was supported by the European Research Council Grant “TETHYS” (Grant agreement ID
452 864038) and the Max Planck Society.

453 Acknowledgments

454 The authors gratefully thank Caroline M. Weisman for her helpful comments on how to analyze and
455 interpret HDF probabilities. We thank the Max Planck Computing and Data Facility for access to and
456 support of the HPC infrastructure, as well as the BMBF-funded de.NBI Cloud within the German
457 Network for Bioinformatics Infrastructure (de.NBI) (031A532B, 031A533A, 031A533B, 031A534A,
458 031A535A, 031A537A, 031A537B, 031A537C, 031A537D, 031A538A).

459 Author contributions

460 JB-R, JSL, H-GD and SMC conceived the study. JB-R designed and implemented the software. JB-R and
461 JSL analyzed the data. JB-R, JSL, H-GD and SMC interpreted the data. JB-R, JSL, H-GD and SMC wrote
462 the manuscript.

463 Bibliography

- 464 1. Lupas AN, Ponting CP, Russell RB. On the evolution of protein folds: are similar motifs in different
465 protein folds the result of convergence, insertion, or relics of an ancient peptide world? *J Struct*
466 *Biol.* 2001 Jun;134(2–3):191–203.
- 467 2. Alva V, Remmert M, Biegert A, Lupas AN, Söding J. A galaxy of folds. *Protein Sci.* 2010
468 Jan;19(1):124–30.

- 469 3. Ohno S. Evolution By Gene Duplication. Springer Science & Business Media; 2013.
- 470 4. Tautz D, Domazet-Lošo T. The evolutionary origin of orphan genes. *Nat Rev Genet.* 2011 Aug
471 31;12(10):692–702.
- 472 5. Neme R, Tautz D. Phylogenetic patterns of emergence of new genes support a model of frequent
473 de novo evolution. *BMC Genomics.* 2013 Feb 21;14:117.
- 474 6. Carvunis A-R, Rolland T, Wapinski I, Calderwood MA, Yildirim MA, Simonis N, et al. Proto-genes
475 and de novo gene birth. *Nature.* 2012 Jul 19;487(7407):370–4.
- 476 7. Domazet-Lošo T, Brajković J, Tautz D. A phylostratigraphy approach to uncover the genomic
477 history of major adaptations in metazoan lineages. *Trends Genet.* 2007 Nov;23(11):533–9.
- 478 8. Bowles AMC, Bechtold U, Paps J. The origin of land plants is rooted in two bursts of genomic
479 novelty. *Curr Biol.* 2020 Feb 3;30(3):530-536.e2.
- 480 9. Paps J, Holland PWH. Reconstruction of the ancestral metazoan genome reveals an increase in
481 genomic novelty. *Nat Commun.* 2018 Apr 30;9(1):1730.
- 482 10. Dornburg A, Yoder JA. On the relationship between extant innate immune receptors and the
483 evolutionary origins of jawed vertebrate adaptive immunity. *Immunogenetics.* 2022
484 Feb;74(1):111–28.
- 485 11. Baalsrud HT, Tørresen OK, Solbakken MH, Salzburger W, Hanel R, Jakobsen KS, et al. De novo
486 gene evolution of antifreeze glycoproteins in codfishes revealed by whole genome sequence
487 data. *Mol Biol Evol.* 2018 Mar 1;35(3):593–606.
- 488 12. Dohmen E, Klasberg S, Bornberg-Bauer E, Perrey S, Kemena C. The modular nature of protein
489 evolution: domain rearrangement rates across eukaryotic life. *BMC Evol Biol.* 2020 Feb
490 14;20(1):30.
- 491 13. Moyers B, Zhang J. Phylostratigraphic bias creates spurious patterns of genome evolution. *Mol
492 Biol Evol.* 2016 Nov;33(11):3031.
- 493 14. Moyers BA, Zhang J. Further simulations and analyses demonstrate open problems of
494 phylostratigraphy. *Genome Biol Evol.* 2017 Jun 1;9(6):1519–27.
- 495 15. Weisman CM, Murray AW, Eddy SR. Many, but not all, lineage-specific genes can be explained
496 by homology detection failure. *PLoS Biol.* 2020 Nov 2;18(11):e3000862.
- 497 16. Lewin HA, Robinson GE, Kress WJ, Baker WJ, Coddington J, Crandall KA, et al. Earth BioGenome
498 Project: Sequencing life for the future of life. *Proc Natl Acad Sci USA.* 2018 Apr 24;115(17):4325–
499 33.
- 500 17. Buchfink B, Reuter K, Drost H-G. Sensitive protein alignments at tree-of-life scale using
501 DIAMOND. *Nat Methods.* 2021 Apr 7;18(4):366–8.
- 502 18. de Mendoza A, Sebé-Pedrós A, Šestak MS, Matejčić M, Torruella G, Domazet-Lošo T, et al.
503 Transcription factor evolution in eukaryotes and the assembly of the regulatory toolkit in
504 multicellular lineages. *Proc Natl Acad Sci USA.* 2013 Dec 10;110(50):E4858–66.
- 505 19. Domazet-Lošo T, Tautz D. A phylogenetically based transcriptome age index mirrors ontogenetic
506 divergence patterns. *Nature.* 2010 Dec 9;468(7325):815–8.

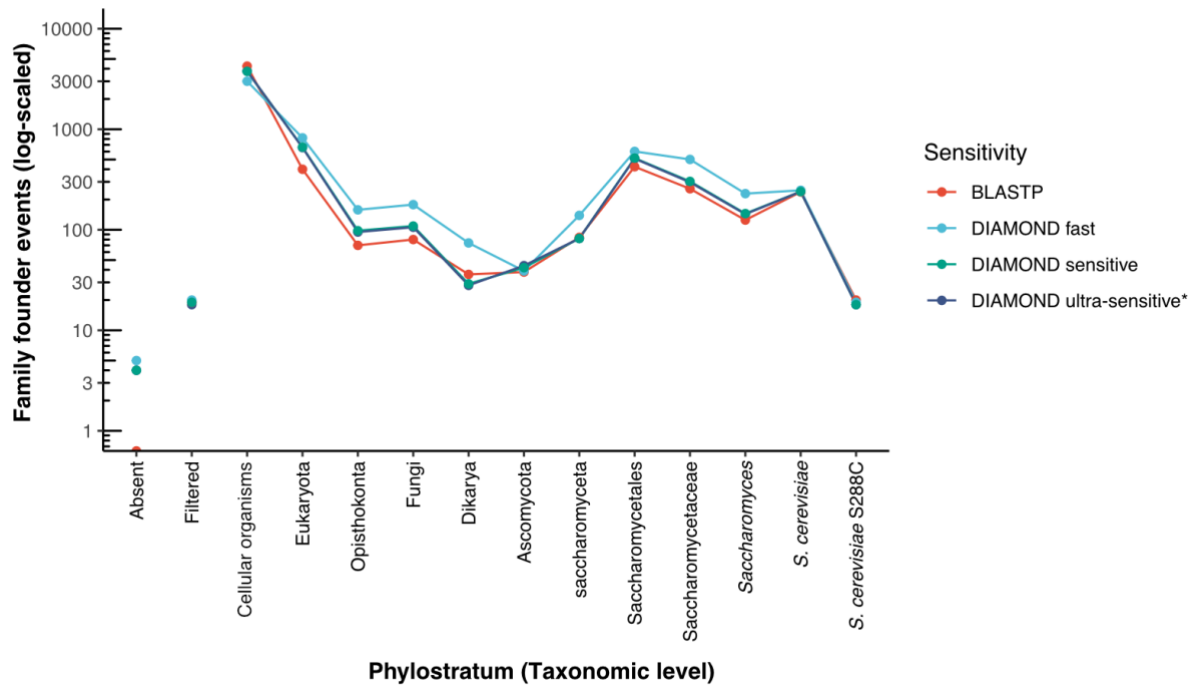
- 507 20. Drost H-G, Janitza P, Grosse I, Quint M. Cross-kingdom comparison of the developmental
508 hourglass. *Curr Opin Genet Dev*. 2017 Aug;45:69–75.
- 509 21. Moutinho AF, Eyre-Walker A, Dutheil JY. Testing the adaptive walk model of gene evolution.
510 *BioRxiv*. 2021 Apr 29;
- 511 22. Casola C. From De Novo to “De Nono”: The Majority of Novel Protein-Coding Genes Identified
512 with Phylostratigraphy Are Old Genes or Recent Duplicates. *Genome Biol Evol*. 2018 Nov
513 1;10(11):2906–18.
- 514 23. Weisman CM, Murray AW, Eddy SR. Mixing genome annotation methods in a comparative
515 analysis inflates the apparent number of lineage-specific genes. *Curr Biol*. 2022 May 12;
- 516 24. Arendsee Z, Li J, Singh U, Seetharam A, Dorman K, Wurtele ES. phylostratr: a framework for
517 phylostratigraphy. *Bioinformatics*. 2019 Oct 1;35(19):3617–27.
- 518 25. James JE, Willis SM, Nelson PG, Weibel C, Kosinski LJ, Masel J. Universal and taxon-specific trends
519 in protein sequences as a function of age. *eLife*. 2021 Jan 8;10.
- 520 26. Camacho C, Coulouris G, Avagyan V, Ma N, Papadopoulos J, Bealer K, et al. BLAST+: architecture
521 and applications. *BMC Bioinformatics*. 2009 Dec 15;10:421.
- 522 27. Domazet-Lošo T, Carvunis A-R, Albà MM, Šestak MS, Bakaric R, Neme R, et al. No evidence for
523 phylostratigraphic bias impacting inferences on patterns of gene emergence and evolution. *Mol*
524 *Biol Evol*. 2017 Apr 1;34(4):843–56.
- 525 28. Moyers BA, Zhang J. Toward reducing phylostratigraphic errors and biases. *Genome Biol Evol*.
526 2018 Aug 1;10(8):2037–48.
- 527 29. Johnson LS, Eddy SR, Portugaly E. Hidden Markov model speed heuristic and iterative HMM
528 search procedure. *BMC Bioinformatics*. 2010 Aug 18;11:431.
- 529 30. Altschul SF, Madden TL, Schäffer AA, Zhang J, Zhang Z, Miller W, et al. Gapped BLAST and PSI-
530 BLAST: a new generation of protein database search programs. *Nucleic Acids Res*. 1997 Sep
531 1;25(17):3389–402.
- 532 31. Basile W, Elofsson A. The number of orphans in yeast and fly is drastically reduced by using
533 combining searches in both proteomes and genomes. *BioRxiv*. 2017 Sep 7;
- 534 32. Arendsee Z, Li J, Singh U, Bhandary P, Seetharam A, Wurtele ES. fagin: synteny-based
535 phylostratigraphy and finer classification of young genes. *BMC Bioinformatics*. 2019 Aug
536 27;20(1):440.
- 537 33. Engel SR, Dietrich FS, Fisk DG, Binkley G, Balakrishnan R, Costanzo MC, et al. The reference
538 genome sequence of *Saccharomyces cerevisiae*: then and now. *G3 (Bethesda)*. 2014 Mar
539 20;4(3):389–98.
- 540 34. Chen L, Wiens JJ. Multicellularity and sex helped shape the Tree of Life. *Proc Biol Sci*. 2021 Jul
541 28;288(1955):20211265.
- 542 35. Schoch CL, Ciuffo S, Domrachev M, Hottton CL, Kannan S, Khovanskaya R, et al. NCBI Taxonomy: a
543 comprehensive update on curation, resources and tools. *Database (Oxford)*. 2020 Jan 1;2020.
- 544 36. Steinegger M, Söding J. MMseqs2 enables sensitive protein sequence searching for the analysis
545 of massive data sets. *Nat Biotechnol*. 2017 Nov;35(11):1026–8.

- 546 37. Sakamoto T, Ortega JM. Taxallnomy: an extension of NCBI Taxonomy that produces a
547 hierarchically complete taxonomic tree. *BMC Bioinformatics*. 2021 Jul 29;22(1):388.
- 548 38. del Campo J, Sieracki ME, Molestina R, Keeling P, Massana R, Ruiz-Trillo I. The others: our biased
549 perspective of eukaryotic genomes. *Trends Ecol Evol*. 2014 May;29(5):252–9.
- 550 39. Assis LCS, Rieppel O. Are monophyly and synapomorphy the same or different? Revisiting the
551 role of morphology in phylogenetics. *Cladistics*. 2011 Feb;27(1):94–102.
- 552 40. Enright AJ, Van Dongen S, Ouzounis CA. An efficient algorithm for large-scale detection of protein
553 families. *Nucleic Acids Res*. 2002 Apr 1;30(7):1575–84.
- 554 41. Laumer CE, Fernández R, Lemer S, Combosch D, Kocot KM, Riesgo A, et al. Revisiting metazoan
555 phylogeny with genomic sampling of all phyla. *Proc Biol Sci*. 2019 Jul 10;286(1906):20190831.
- 556 42. Paradis E, Schliep K. ape 5.0: an environment for modern phylogenetics and evolutionary
557 analyses in R. *Bioinformatics*. 2019 Feb 1;35(3):526–8.
- 558 43. Li Y, Steenwyk JL, Chang Y, Wang Y, James TY, Stajich JE, et al. A genome-scale phylogeny of the
559 kingdom Fungi. *Curr Biol*. 2021 Apr 26;31(8):1653–1665.e5.
- 560 44. King N, Westbrook MJ, Young SL, Kuo A, Abedin M, Chapman J, et al. The genome of the
561 choanoflagellate *Monosiga brevicollis* and the origin of metazoans. *Nature*. 2008 Feb
562 14;451(7180):783–8.
- 563 45. One Thousand Plant Transcriptomes Initiative. One thousand plant transcriptomes and
564 the phylogenomics of green plants. *Nature*. 2019 Oct 23;574(7780):679–85.
- 565 46. Umen JG. Green algae and the origins of multicellularity in the plant kingdom. *Cold Spring Harb
566 Perspect Biol*. 2014 Oct 16;6(11):a016170.
- 567 47. Rensing SA. Great moments in evolution: the conquest of land by plants. *Curr Opin Plant Biol*.
568 2018 Apr;42:49–54.
- 569 48. Chanderbali AS, Berger BA, Howarth DG, Soltis PS, Soltis DE. Evolving ideas on the origin and
570 evolution of flowers: new perspectives in the genomic era. *Genetics*. 2016 Apr;202(4):1255–65.
- 571 49. Pires N, Dolan L. Origin and diversification of basic-helix-loop-helix proteins in plants. *Mol Biol
572 Evol*. 2010 Apr;27(4):862–74.
- 573 50. Roudier F, Schindelman G, DeSalle R, Benfey PN. The COBRA family of putative GPI-anchored
574 proteins in *Arabidopsis*. A new fellowship in expansion. *Plant Physiol*. 2002 Oct;130(2):538–48.
- 575 51. Prabhakaran Mariyamma N, Clarke KJ, Yu H, Wilton EE, Van Dyk J, Hou H, et al. Members of the
576 *Arabidopsis* FORKED1-LIKE gene family act to localize PIN1 in developing veins. *J Exp Bot*. 2018
577 Sep 14;69(20):4773–90.
- 578 52. Fan C, Guo G, Yan H, Qiu Z, Liu Q, Zeng B. Characterization of Brassinazole resistant (BZR) gene
579 family and stress induced expression in *Eucalyptus grandis*. *Physiol Mol Biol Plants*. 2018
580 Sep;24(5):821–31.
- 581 53. Zhang X, Gou M, Liu C-J. *Arabidopsis* Kelch repeat F-box proteins regulate phenylpropanoid
582 biosynthesis via controlling the turnover of phenylalanine ammonia-lyase. *Plant Cell*. 2013 Dec
583 20;25(12):4994–5010.

- 584 54. Banerjee A, Roychoudhury A. Group II late embryogenesis abundant (LEA) proteins: structural
585 and functional aspects in plant abiotic stress. *Plant Growth Regul.* 2016 May;79(1):1–17.
- 586 55. van Dop M, Fiedler M, Mutte S, de Keijzer J, Olijslager L, Albrecht C, et al. DIX domain
587 polymerization drives assembly of plant cell polarity complexes. *Cell.* 2020 Feb 6;180(3):427-
588 439.e12.
- 589 56. Lee YK, Kim G-T, Kim I-J, Park J, Kwak S-S, Choi G, et al. LONGIFOLIA1 and LONGIFOLIA2, two
590 homologous genes, regulate longitudinal cell elongation in Arabidopsis. *Development.* 2006
591 Nov;133(21):4305–14.
- 592 57. Zhang L, Ren Y, Yang T, Li G, Chen J, Gschwend AR, et al. Rapid evolution of protein diversity by
593 de novo origination in *Oryza*. *Nat Ecol Evol.* 2019 Apr;3(4):679–90.
- 594 58. Su M, Ling Y, Yu J, Wu J, Xiao J. Small proteins: untapped area of potential biological importance.
595 *Front Genet.* 2013 Dec 16;4:286.
- 596 59. Jones S. An overview of the basic helix-loop-helix proteins. *Genome Biol.* 2004 May 28;5(6):226.
- 597 60. Moody LA, Saidi Y, Gibbs DJ, Choudhary A, Holloway D, Vesty EF, et al. An ancient and conserved
598 function for Armadillo-related proteins in the control of spore and seed germination by abscisic
599 acid. *New Phytol.* 2016 Aug;211(3):940–51.
- 600 61. Mittal A, Singh S. Insights into eukaryotic evolution from transmembrane domain lengths. *J*
601 *Biomol Struct Dyn.* 2018 Jun;36(8):2194–200.
- 602 62. Keeling DM, Garza P, Nartey CM, Carvunis A-R. The meanings of “function” in biology and the
603 problematic case of de novo gene emergence. *eLife.* 2019 Nov 1;8.
- 604 63. Knoll AH. The Multiple Origins of Complex Multicellularity. *Annu Rev Earth Planet Sci.* 2011 May
605 30;39(1):217–39.
- 606 64. Pagel M, Venditti C, Meade A. Large punctuational contribution of speciation to evolutionary
607 divergence at the molecular level. *Science.* 2006 Oct 6;314(5796):119–21.
- 608 65. Barraclough TG, Savolainen V. Evolutionary rates and species diversity in flowering plants.
609 *Evolution.* 2007 May 9;55(4):677–83.
- 610 66. Lanfear R, Ho SYW, Love D, Bromham L. Mutation rate is linked to diversification in birds. *Proc*
611 *Natl Acad Sci USA.* 2010 Nov 23;107(47):20423–8.
- 612 67. Hua X, Bromham L. Darwinism for the genomic age: connecting mutation to diversification. *Front*
613 *Genet.* 2017 Feb 7;8:12.
- 614 68. Sebé-Pedrós A, Roger AJ, Lang FB, King N, Ruiz-Trillo I. Ancient origin of the integrin-mediated
615 adhesion and signaling machinery. *Proc Natl Acad Sci USA.* 2010 Jun 1;107(22):10142–7.
- 616 69. Nagy LG, Varga T, Csérnetics Á, Virágh M. Fungi took a unique evolutionary route to
617 multicellularity: Seven key challenges for fungal multicellular life. *Fungal Biol Rev.* 2020 Aug;
- 618 70. Neuman-Silberberg FS, Schüpbach T. The *Drosophila* TGF- α -like protein Gurken: expression
619 and cellular localization during *Drosophila* oogenesis. *Mech Dev.* 1996 Oct;59(2):105–13.
- 620 71. Rutledge BJ, Zhang K, Bier E, Jan YN, Perrimon N. The *Drosophila* spitz gene encodes a putative
621 EGF-like growth factor involved in dorsal-ventral axis formation and neurogenesis. *Genes Dev.*

- 622 1992 Aug;6(8):1503–17.
- 623 72. Liu J, Ma J. Dampened regulates the activating potency of Bicoid and the embryonic patterning
624 outcome in *Drosophila*. *Nat Commun*. 2013;4:2968.
- 625 73. Lee KJ, Freeman M, Steller H. Expression of the disconnected gene during development of
626 *Drosophila melanogaster*. *EMBO J*. 1991 Apr;10(4):817–26.
- 627 74. Clark JW, Donoghue PCJ. Whole-Genome Duplication and Plant Macroevolution. *Trends Plant*
628 *Sci*. 2018 Oct;23(10):933–45.
- 629 75. Pertseva M. The evolution of hormonal signalling systems. *Comp Biochem Physiol A Comp*
630 *Physiol*. 1991;100(4):775–87.
- 631 76. Ornelas-Ayala D, Garay-Arroyo A, García-Ponce B, R Álvarez-Buylla E, Sanchez M de la P. The
632 epigenetic faces of ULTRAPETALA1. *Front Plant Sci*. 2021 Feb 25;12:637244.
- 633 77. Schuettengruber B, Martinez A-M, Iovino N, Cavalli G. Trithorax group proteins: switching genes
634 on and keeping them active. *Nat Rev Mol Cell Biol*. 2011 Nov 23;12(12):799–814.
- 635 78. Tam THY, Catarino B, Dolan L. Conserved regulatory mechanism controls the development of
636 cells with rooting functions in land plants. *Proc Natl Acad Sci USA*. 2015 Jul 21;112(29):E3959-68.
- 637 79. Lan P, Li W, Lin W-D, Santi S, Schmidt W. Mapping gene activity of *Arabidopsis* root hairs. *Genome*
638 *Biol*. 2013 Jun 25;14(6):R67.
- 639 80. Shahollari B, Vadassery J, Varma A, Oelmüller R. A leucine-rich repeat protein is required for
640 growth promotion and enhanced seed production mediated by the endophytic fungus
641 *Piriformospora indica* in *Arabidopsis thaliana*. *Plant J*. 2007 Apr;50(1):1–13.
- 642 81. Gramzow L, Ritz MS, Theissen G. On the origin of MADS-domain transcription factors. *Trends*
643 *Genet*. 2010 Apr;26(4):149–53.
- 644 82. Wang S, Chang Y, Guo J, Zeng Q, Ellis BE, Chen J-G. *Arabidopsis* ovate family proteins, a novel
645 transcriptional repressor family, control multiple aspects of plant growth and development. *PLoS*
646 *ONE*. 2011 Aug 23;6(8):e23896.
- 647

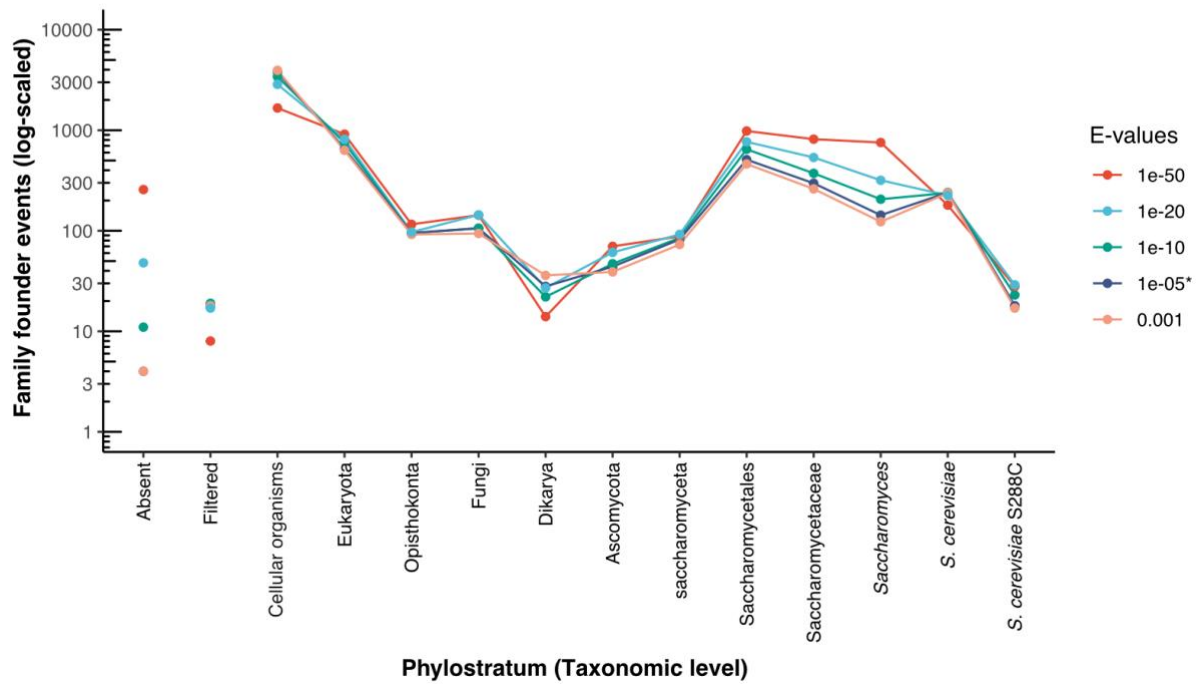
648 Supplementary figures



649

650 **Figure S1. Impact of DIAMOND search sensitivity level on gene age assignment in *S. cerevisiae* while using BLASTP**
651 **as reference.** DIAMOND in ultra-sensitive and sensitive mode generates a similar pattern of gene age assignment
652 as the gold-standard of BLASTP while using the same e-value threshold of $1e^{-5}$. DIAMOND in fast mode assigns
653 younger ages to genes compared to more sensitive modes as a consequence of not finding as many distantly
654 related homolog genes in the database. The search sensitivity level does not influence the number of genes that
655 are filtered through the taxonomic representativeness threshold (filtered; values below 30% taxonomic
656 representativeness), and has a negligible effect on the number of genes that fail to match themselves through
657 pairwise alignment (absent). We established ultra-sensitive as the default sensitivity mode for GenEra (asterisk).

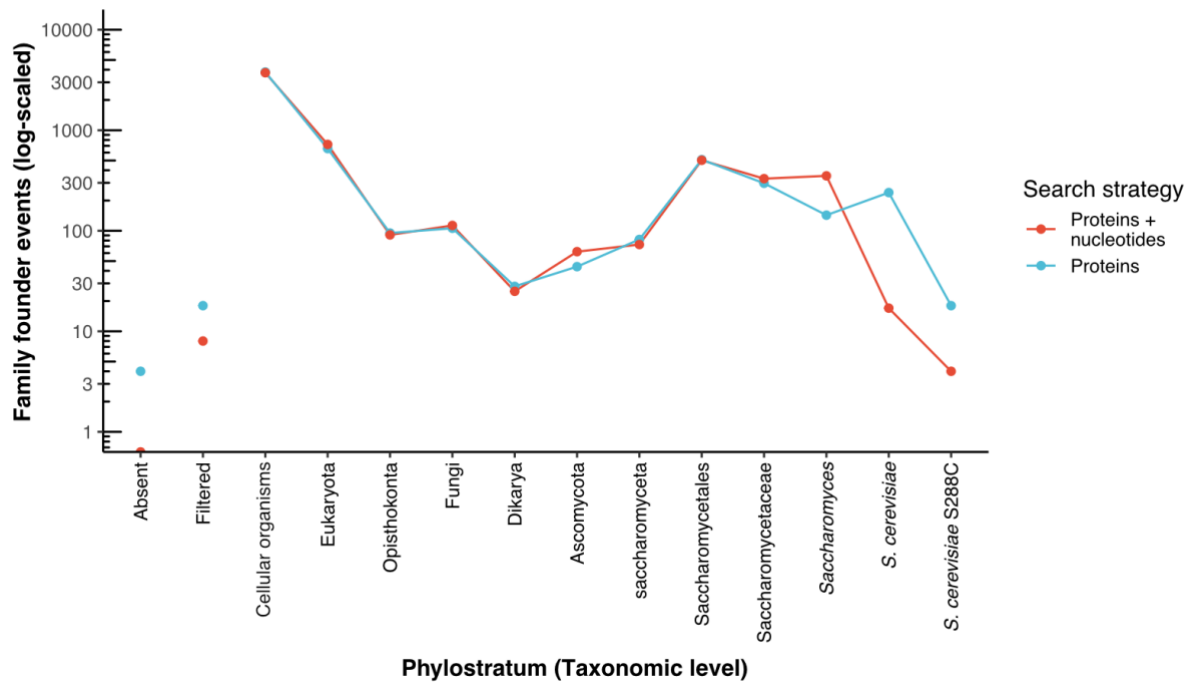
658



659

660 **Figure S2. Impact of e-value thresholds on gene age assignments in *S. cerevisiae*.** The patterns of gene age
661 assignment remain largely unaffected between a permissive e-value threshold of $1e^{-3}$ and a more stringent
662 threshold of $1e^{-5}$. Using more stringent thresholds ($1e^{-10}$ or lower) leads to an overrepresentation of TRGs at
663 younger taxonomic levels. Lower e-value thresholds also increase the amount of genes whose self-alignment
664 cannot be detected (absent), likely increasing the amount of false negative matches in the database. The e-value
665 threshold also has a small influence on the proportion of genes that are discarded through the taxonomic
666 representativeness threshold (filtered; values below 30% taxonomic representativeness). We established a
667 default e-value threshold of $1e^{-5}$ for GenEra (asterisk).

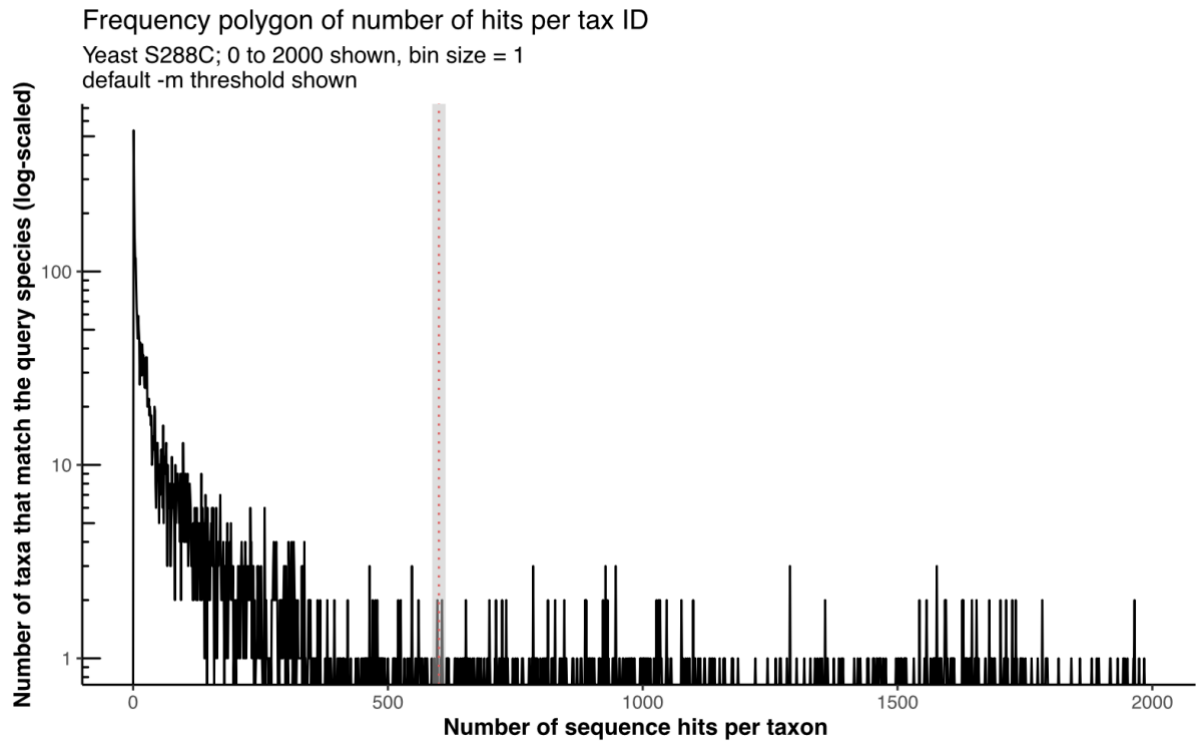
668



669

670 **Figure S3. Impact of using a protein-vs-nucleotide search in addition to predicted gene annotations for the gene**
671 **age assignments of *S. cerevisiae*.** The standard gene age assignment was performed against the predicted genes
672 in the NR, while the protein-vs-nucleotide search includes additional six-frame alignments against 8
673 representative genome assemblies from each taxonomic level, adding to a total of 80 genomes (see Table S1).
674 The age assignment of the youngest genes are pushed to older taxonomic levels, suggesting that young gene age
675 assignments can be overestimated when not taking annotation errors into account. However, older gene age
676 assignments remain largely unaffected by annotation errors, demonstrating that protein-vs-nucleotide searches
677 are mostly impactful over recent gene-family founder events. The taxonomic representativeness also improves
678 when doing a protein-vs-nucleotide search, reducing the number of filtered gene age assignments.

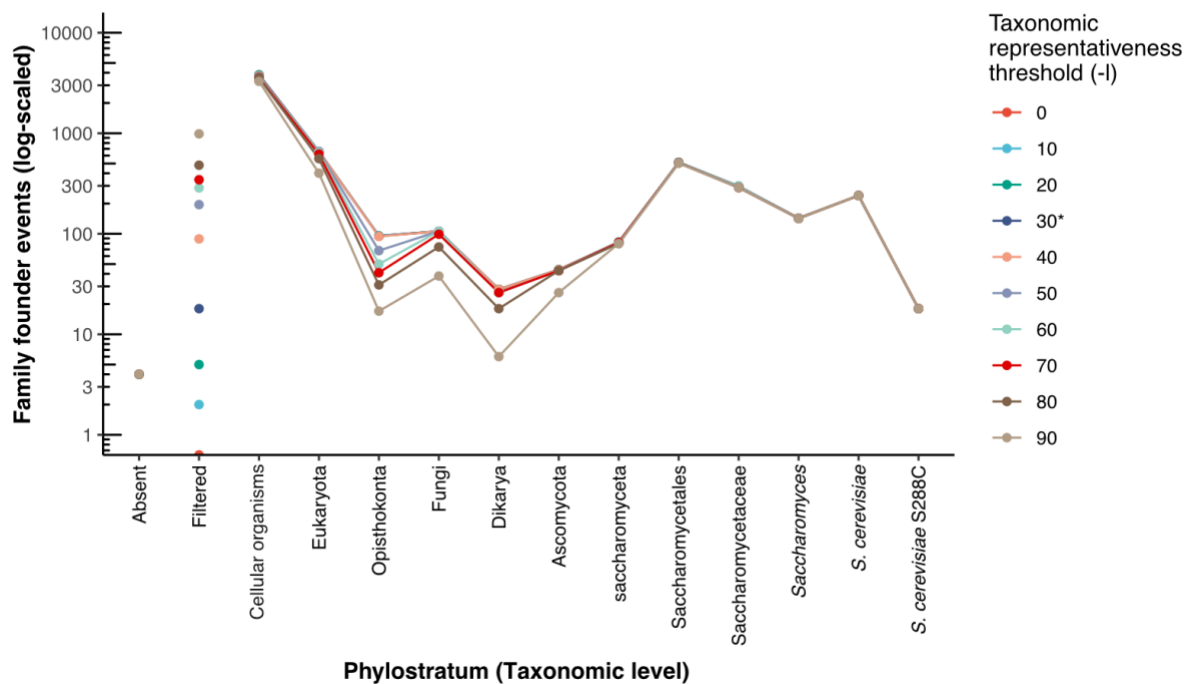
679



680

681 **Figure S4. Distribution of taxa in the NR with sequence matches against the proteome of *S. cerevisiae*.** Most of
682 the taxa in the NCBI non-redundant database contain 50 or less proteins (*e.g.*, sequence data generated for
683 phylogenetic studies), which could lead to an unreliable gene age assignment. An empirical threshold of 10% total
684 hits against the query proteome can successfully detect these cases (red dashed line). This allows GenEra to assign
685 ages only to the taxonomic levels where genomic data is available.

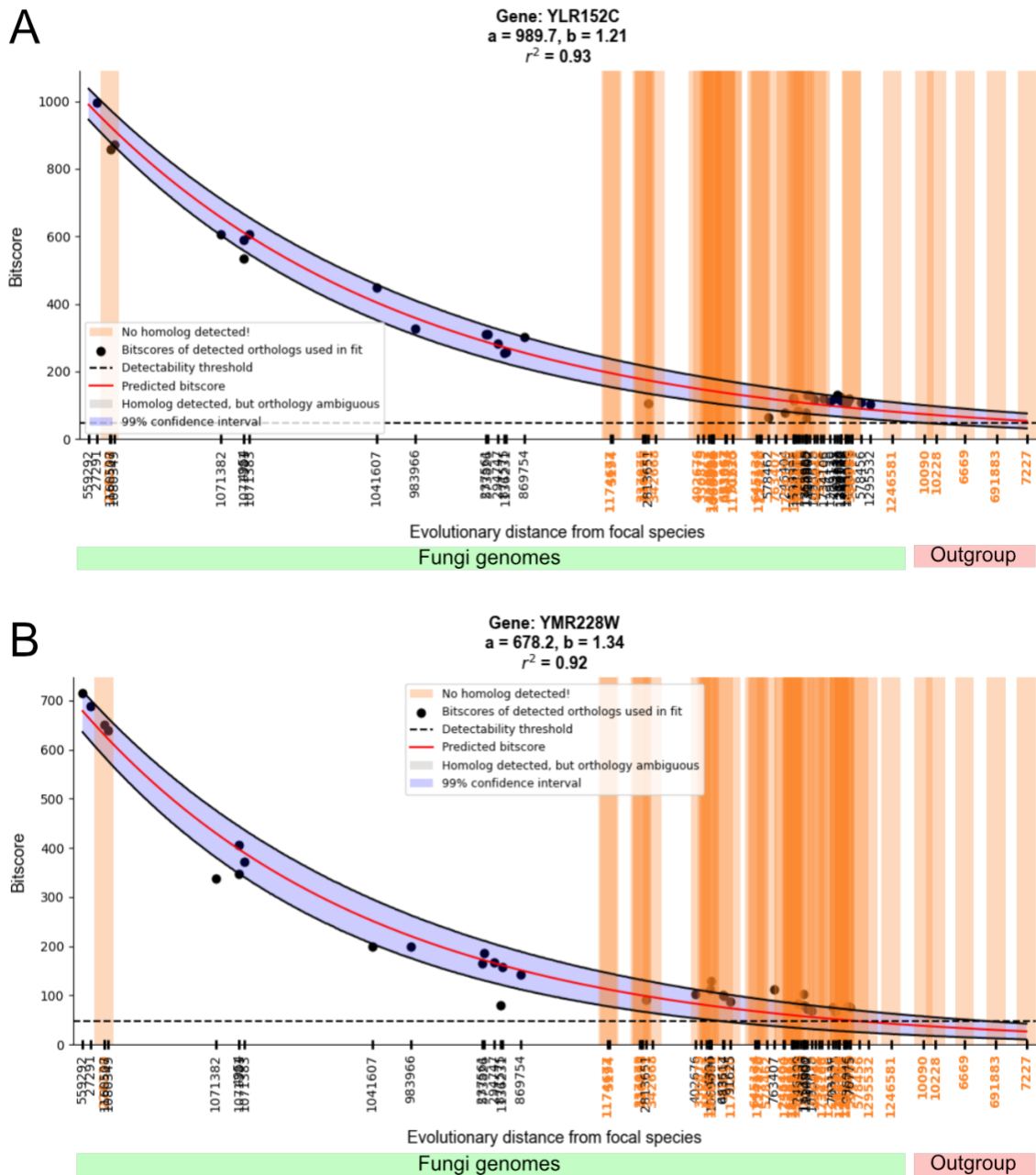
686



687

688 **Figure S5. Assessment of different thresholds for the taxonomic representativeness score in *S. cerevisiae*.** Higher
 689 thresholds have a direct impact on the amount of genes that cannot be assigned to a specific age (filtered). We
 690 established a default threshold of 30% for gene age assignment in GenEra, as lower values of taxonomic
 691 representativeness are bound to represent artifacts due to genome contamination or false positive matches,
 692 while establishing a more stringent threshold would fail to account for gene loss events, influencing the overall
 693 trends of gene age assignments. We established a taxonomic representativeness of 30% as the default threshold
 694 to filter ambiguous gene age assignments (asterisk).

695



696

697 **Figure S6. Decoupling high-confidence gene age assignments from HDF.** Bitscore decay plots as a function of
 698 evolutionary distance in two genes of *S. cerevisiae* across different fungal species (green bar) and other closely
 699 related opisthokonts (red bar). Each species in the horizontal axis is represented by its NCBI Taxonomy ID. The
 700 bitscore values were retrieved from a DIAMOND search against the NR using GenEra, while the pairwise
 701 evolutionary distances (substitutions per site) were retrieved from a previously published maximum likelihood
 702 tree (43). The bitscore prediction and the detection failure probabilities were calculated using abSENSE (15). A)
 703 Bitscore decay of the gene YLR152C, which shows homolog genes across the Fungi kingdom and is predicted to
 704 have detectable bitscore values in *Fonticula alba* and in other closely-related animal genomes (detection failure
 705 probability of 0.01 in the outgroup species). This gene is thereby regarded as a high-confidence fungal TRG. B)
 706 Bitscore decay of the gene YMR228W, which is found within the Fungi kingdom, but whose expected bitscore falls
 707 below the detectability threshold (dashed line) in *Fonticula alba* and in other closely-related animal genomes
 708 (detection failure probability of 1 in the outgroup species). Therefore, the seeming absence of this gene outside
 709 the Fungi kingdom can be explained by HDF.